Applied Physics B (2019) 125:200
https://doi.org/10.1007/s00340-019-7318-5

Applied Physics B
Lasers and Optics

515 nm pumped femtosecond optical parametric oscillator at 755 MHz based on BiB_3O_6

Xianghao Meng[1,3] · Zhaohua Wang[1] · Wenlong Tian[2] · Jiajun Song[1,3] · Xianzhi Wang[1,3] · Jiangfeng Zhu[2] · Zhiyi Wei[1,3,4]

Received: 23 July 2019 / Accepted: 27 September 2019

Abstract
We report a high-power femtosecond optical parametric oscillator (OPO) based on BiB_3O_6 crystal with a repetition rate of 755 MHz, which is 10 times that of the pump laser. With 3.75 W pump power from a 90 fs frequency-doubled mode-locked Yb:KGW oscillator, the OPO can provide signal pulses tunable over a spectral range from 693 to 1000 nm and idler pulses tunable from 1100 to 2000 nm. The maximum signal output power is 1.34 W centered at 746 nm and the corresponding idler output power is 0.408 W at 1663 nm. Laser pulse as short as 67 fs is obtained at the central wavelength of 722 nm. This work is promising for a variety of applications in optical communications and pump-probe spectroscopy.

1 Introduction

High-power wavelength-tunable femtosecond laser sources with multigigahertz repetition rate are becoming valuable tools in time-resolved spectroscopy [1], pump-probe measurements [2], nonlinear optics [3] and high-precision distance measurement [4]. The femtosecond lasers operated in the near-IR region can be employed in ultrafast optical communication systems to achieve high data rates and high capacity. Optical frequency combs from high repetition rate femtosecond lasers featuring high precision and low noise are widely used in numerous frontier research areas, such as optical frequency metrology and optical atomic clock. With the advances in the development of various nonlinear crystals and the techniques of generating femtosecond lasers, nonlinear frequency conversion technology becomes promising to produce continuous wavelength-tunable ultrashort pulse [5–8]. Synchronously pumped optical parametric oscillator (OPO) offers one of the most attractive methods to generate coherent tunable ultrashort pulse ubiquitously from the UV to the mid-infrared owing to its extremely broad tuning range and wide gain bandwidth [9–14]. Several methods have been investigated to generate pulse trains with high repetition rate, such as harmonic pumping scheme. In 1997, Reid et al. first report a 344 MHz RTA OPO pumped by a Kerr-lens mode-locked (KLM) Ti:saphhire laser operated at 86 MHz [15]. Three years later, Phillips et al. demonstrated a 322 MHz femtosecond PPLN OPO harmonically pumped by a mode-locked 84 MHz Ti:sapphire laser [16]. For harmonically pumped OPOs, it is possible to employ a low-frequency laser pulse train to pump an OPO to generate high repetition rate laser pulse by matching the cavity length between the pump and OPO [17]. When the effective OPO cavity length $L_{OPO} = L_{PUMP}/N$ (N is an integer) is chosen, the repetition rate of OPO can thus be multiplied by a factor of N. Compared to synchronously pumping, harmonic pumping is more flexible because a lower repetition rate pulse trains can generate a much higher single pulse energy to exceed the threshold peak power intensity necessary for pumping an OPO. However, the signal pulses have periodically varying intensities because the gain is not provided for each pass through the crystal. The signal pulses experience more round-trip losses, and the corresponding pump threshold is increased. The progress in harmonically

✉ Zhaohua Wang
zhwang@iphy.ac.cn

✉ Zhiyi Wei
zywei@iphy.ac.cn

[1] Beijing National Laboratory for Condensed Matter Physics, Institute of Physics, Chinese Academy of Sciences, Beijing 100190, China

[2] School of Physics and Optoelectronic Engineering, Xidian University, Xi'an 710071, China

[3] University of Chinese Academy of Sciences, Beijing 100049, China

[4] Songshan Lake Materials Laboratory, Dongguan 523808, Guangdong, China

Published online: 08 October 2019

pumped femtosecond OPOs is triggered with the invention of KLM Ti:sapphire lasers. Limited mainly by the pump sources, the output power of signal is low and tuning range is reduced. Recently, high-power ytterbium-doped (Yb-doped) solid-state femtosecond oscillators and fiber amplifiers offer attractive properties for OPOs [18–24]. In 2011, Cleff et al. report a femtosecond PPLN OPO synchronously pumped by a frequency-doubled Yb-fiber amplifier [25]. The signal wavelengths are tunable from 780–940 nm with the output power more than 250 mW. Several years later, Gu et al. reported a dual-wavelength femtosecond LiB_3O_5 (LBO) OPO synchronously pumped by a frequency-doubled 57 MHz Yb-fiber amplifier [26]. The dual wavelength operation is achieved over the ranges of 658–846 nm and 2.45–1.35 μm. In 2016, we have demonstrated a high-power femtosecond OPO based on BiB_3O_6 (BIBO) crystal at repetition rate of 151-MHz, which is twice that of the pump laser [27]. Compared to β-BaB_2O_4 (BBO) and LBO, the effective nonlinear coefficient of BIBO is about 3.7 pm/V, which is nearly twice larger than BBO and four times larger than LBO. Larger effective nonlinear coefficient allows the femtosecond BIBO OPO to run at much lower pump threshold. Low-pump threshold allows much higher repetition rate operation of the corresponding OPOs. Although the effective nonlinear coefficient of BIBO is lower than PPLN or PPKTP, the BIBO crystal combines high optical damage threshold with substantially larger optical nonlinearity and lower group velocity dispersion, which is the advantage for high-power short pulse generation.

In this letter, we report a 755-MHz femtosecond BIBO OPO harmonically pumped by a frequency-doubled mode-locked Yb:KGW laser. Using a 2.4-mm-long BIBO, the signal wavelength can be tuned from 693 to 1000 nm, with a tunable idler wavelength range of 1100–2000 nm by angle tuning and optimizing the cavity length. The OPO delivers as much as 1.34 W of output power at 746 nm with a 35.7% conversion efficiency for signal. Simultaneously, the output power of idler is 408 mW at 1663 nm and the corresponding conversion efficiency is 10.9%. By implementing dispersion control, nearly transform-limited signal pulse of 67 fs duration is achieved at 722 nm. The signal powers have a power drift value of 2.3% over 30 min.

2 Experiment setup

The schematic diagram of 755 MHz BIBO OPO setup is shown in Fig. 1. A frequency-doubled mode-locked Yb:KGW laser (Light Conversion, FLINT 6.0) providing 3.75 W of power at 515 nm is used as the pump source. The repetition rate of the pump laser is 75.5 MHz with a pulse duration of 90 fs. The resonator of the OPO is chosen to be a ring cavity to reduce the signal loss and the optical feedback problem [28]. The four-mirror folded ring cavity is formed by two concave mirrors (C1 and C2) with radius of curvature, $r = 100$ mm, a plane mirror (HR), and an output coupler (OC). The two curved mirrors have a reflectivity of 99.9% centered at the signal wavelength (670–1020 nm) and a transmissivity of 99.5% at the 500–550 nm pump wavelength. The OC with 3% transmission is chosen to overcome the large cavity loss of the resonating signal radiation, which is mounted on a piezoelectric transducer (PZT) for fine tuning of the cavity length. A 2.4-mm-long BIBO is used as the nonlinear crystal owing to its relatively large effective nonlinear coefficient. The BIBO crystal is cut for type I ($o \rightarrow e + e$) phase-matching condition in the Y–Z plane ($\theta = 174°$, $\varphi = 90°$), coated with high transmittance in both 510–530 nm and 700–1040 nm region. The repetition rate of the OPO is determined by the cavity length. The total ring cavity length is only 397.5 mm and the roundtrip time of the OPO cavity is one tenth of that of the pump laser cavity, corresponding to 755-MHz-repetition rate, which is 10 times that of the pump source. The incident angle at each mirror is 8°. Based on ABCD propagation matrix, the laser mode waist radius is calculated as 38 μm in the BIBO crystal, which is slightly larger than that of the pump laser.

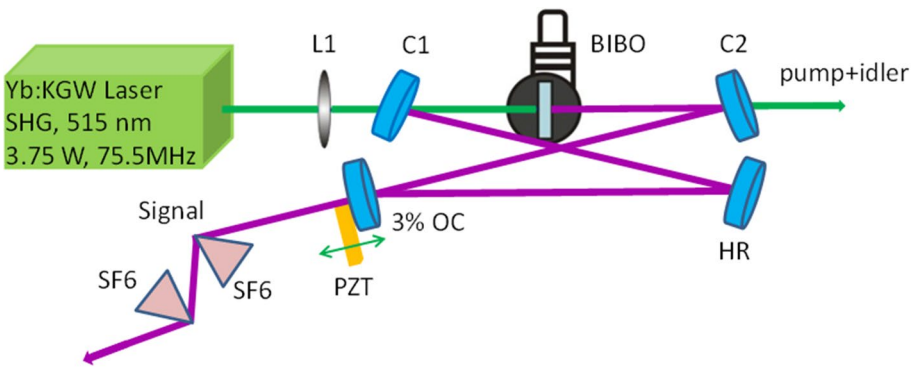

Fig. 1 Experimental setup for 755-MHz femtosecond BIBO OPO. L1: lens, C1, C2: concave spherical mirrors, HR: plane mirror, OC: 3% output coupler, PZT: piezoelectric transducer, SF6: prism

3 Experimental results and discussions

To achieve successful operation of the OPO, the OPO cavity length is satisfied well with the harmonic pumping condition. The wavelength tuning is obtained by rotating the BIBO crystal and optimizing the cavity length. The OPO is almost gap free tunable across 693–1000 nm in the signal and 1100–2000 nm in the idler. Under the pump power of 3.75 W, the maximum measured signal output power is 1.34 W at central wavelength of 746 nm, and the corresponding idler power is 408 mW at 1663 nm. The conversion efficiencies of each beam are 35.7% and 10.9%, respectively. The oscillation is achieved at a pump threshold of 1.7 W with 15 mW of signal power extracted through the 3% OC. Figure 2 shows the output spectra and the corresponding average output powers across the signal and idler tuning range of the femtosecond BIBO OPO. As shown in Fig. 2a, most of the signals across the tuning range are above 250 mW. The output power decreases in the long wavelength around 1030 nm because the operation is caused by the point closing to degeneracy. Figure 2b also shows the output powers for the idler. Because the surface of mirror C2 is not coated with high transmittance for idler, the maximum average power is only 408 mW. The loss of idler power is estimated to reach about 15%. The output powers of idler are more than 100 mW across most of the tuning range.

The group delay dispersion (GDD) induced by the materials has to be carefully analyzed. The GDD between the signals from 690 to 1000 nm and pump of 515 nm for 2.4-mm long BIBO crystal is in the range of 472.6–256.3 fs^2. A pair of chirped mirrors (C1 and C2) with $-200\ fs^2 \pm 30\ fs^2$ GDD (720–1000 nm) for each piece are used to compensate the positive intra-cavity dispersion. We measured the signal pulse duration using a commercial intensity autocorrelator (FR-103MN, Femtochrome Research, Inc). Initially, the pulse durations are measured directly from the OPO, which are in the range of 120–290 fs across the signal tuning range. To obtain nearly transform-limited ultrashort pulses, a pair of SF6 prisms are used for extra-cavity dispersion compensation. Precise dispersion control is achieved by adjusting the insertion of the second prism and changing the prism separation. The tip–tip distance between two prisms is 450 mm. As shown in Fig. 3a, assuming a $sech^2$-pulse shape, the autocorrelation width of the pulse is 67 fs. The

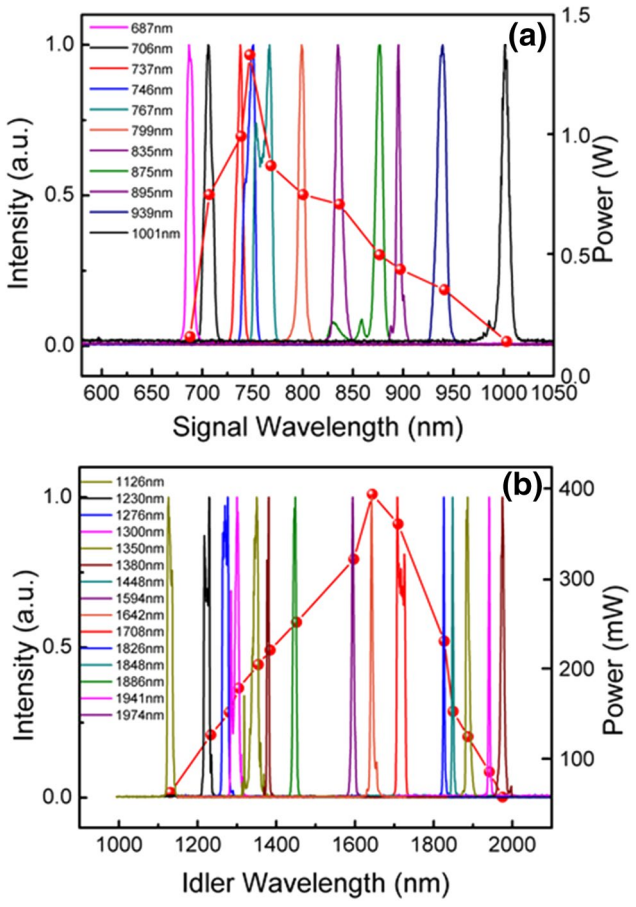

Fig. 2 (Color online) Normalized output spectra and the corresponding average output powers across the tuning range of the 755-MHz femtosecond BIBO OPO: **a** Signal; **b** Idler

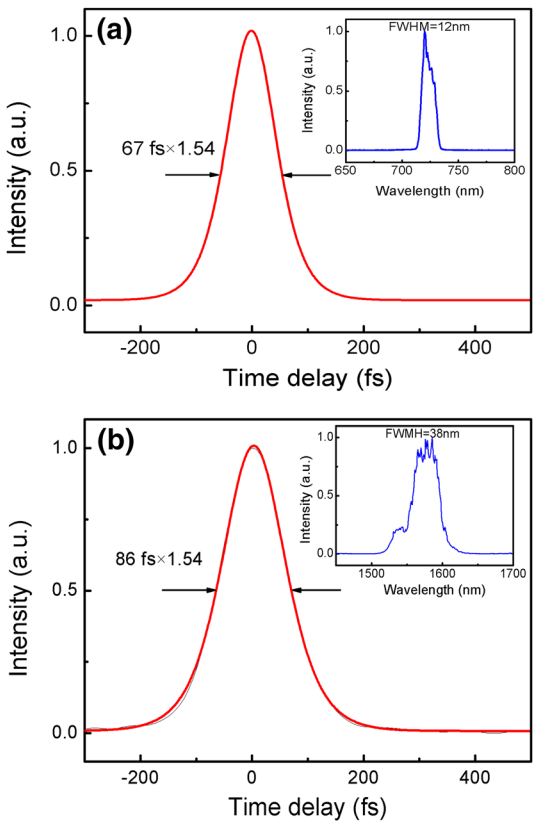

Fig. 3 Typical intensity autocorrelation trace and spectrum: **a** Signal at 722 nm; **b** Idler at 1580 nm

corresponding signal spectrum concentrated at 722 nm is shown in the inset of Fig. 3a, and the transform-limited pulse duration is 46 fs, calculated by Fourier transforming the spectrum without dispersion. These two measurements indicate that the time-bandwidth product ($\Delta\tau$, $\Delta\nu$) is ~ 0.462, implying the signal pulse has a small amount of chirp. Similarly, the pulse duration of idler is also characterized behind C2. Using a commercial intensity autocorrelator (PulseCheck-50, A. P. E. GmbH), as shown in Fig. 3b, the typical intensity autocorrelation trace of the idler pulse at 1580 nm is measured to be 86 fs and the corresponding transform-limited pulse duration is 68 fs calculated from the measured optical spectrum. Within the entire wavelength tuning range, the signal pulse durations are between 67 and 130 fs by compensating extra-cavity dispersion. The short pulse duration is attributed to the broadband crystal phase-matching bandwidth and dispersion compensation.

To characterize the status of the OPO operation, we investigated output signal pulse train and repetition frequency stability of the OPO. The radio frequency (RF) spectra are measured by a 26 GHz spectrum analyzer (Rohde & Schwarz FSW26) with a photodetection. Figure 4a reveals the high harmonics of the fundamental frequency, spanning 1 GHz with a resolution of 100 kHz. The RF spectra appear regular; they are 75.5 MHz apart, which is equal to the repetition rate of the pump laser. The clean RF spectra indicate the perfect synchronization of the OPO repetition rate to the pump laser. As shown in the inset of Fig. 4a, we also measured the repetition rate of the output signal pulses using a photodetector and a fast oscilloscope (1 GHz, 10GS/s DPO5104B, Tektronix), where a repetition rate of 755 MHz, synchronized to the 10th harmonic of the pump laser repetition frequency of 75.5 MHz, is confirmed. The highest peak pulse is the first signal pulse generated in OPO. It is noted that 9 succeeding signal pulses follow them. The peak of first signal pulse is obviously higher than those of the following ones. The intensity of pulse trains takes on a decreasing trend in a period due to the ring-down effect in the ring cavity. The phase noise of high-repetition rate is a particularly relevant parameter for OPO applications. To quantitatively analyze the noise property of signal pulses, we measured the phase noise power spectral density (PSD) by a photodiode and an RF spectrum analyzer (Rohde & Schwarz FSW26). Without the band pass filter, the 755-MHz signal pulse trains include other harmonic frequencies. As Fig. 4b shows, the phase noise mainly comes from the cavity length detuning. The OPO signal pulses present low noise with shot-noise-limited performance (− 135 dB/Hz) from 10 kHz to 1 MHz. The low noise level in high frequency is attributed to the robust all-solid-state pump source. Note that low-frequency phase noise exhibits high noise in the range of 1 Hz–10 kHz, which is caused by the

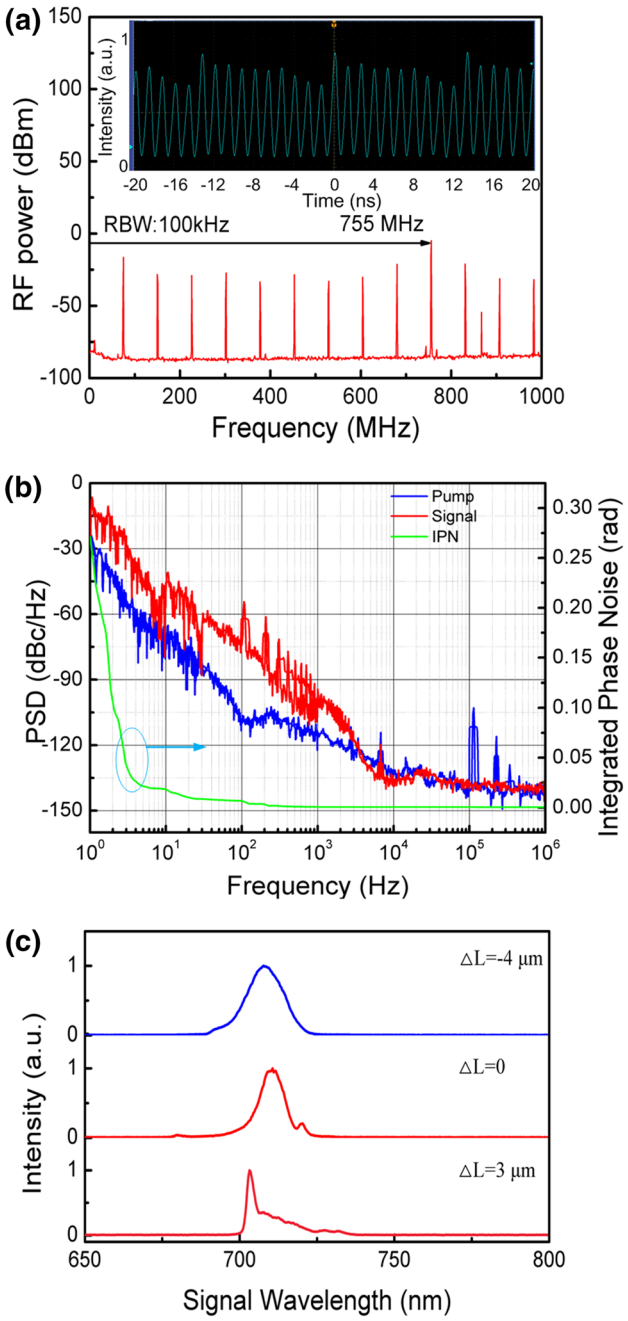

Fig. 4 **a** Typical radio-frequency spectrum from 0 Hz to 1 GHz with 100 kHz resolution. Inset: Pulse train of the 755 MHz signals; **b** Phase noise PSD of signal from 1 Hz to 1 MHz; **c** Signal spectra versus cavity length detuning (ΔL_{OPO})

air disturbance, vibration and temperature drift. Considering that the OPO is directly built on the optical table without any housing, we believe that the noises would be much lower with good housing and active feedback control of the cavity length. However, those methods cannot compensate the phase noise above ~ 10 kHz limited by the component bandwidth. The green curve in Fig. 4b shows

the integrated phase noise of OPO. Thanks to the all-solid-state pump source, the integrated phase noise from 1 Hz to 1 MHz is only 0.26 rad.

The OC mirror of the OPO is mounted on a PZT to enable cavity length tuning. The PZT is driven by a sawtooth function with an amplitude of 75 V. Figure 4c shows the signal spectra versus cavity length detuning (ΔL_{OPO}); the OPO remains operation within only about 7 μm of cavity length mismatch. The cavity length variation results in central wavelength shift of the signal pulses as a result of positive cavity GDD. Within the tolerance of cavity length tuning, the highest signal power is about 743 mW at 712 nm. By only cavity length tuning, the signal wavelength can be tuned within a narrow range. The largest bandwidth appears when the ΔL_{OPO} is near 0. It can be inferred that there is a large variation of the pulse duration over the tuning range and the shortest pulse really appears at the largest bandwidth as expected.

Finally, we also measured the long-term power stability and spatial profile of the signal beam at 746 nm. As shown in Fig. 5a, the OPO is recorded to exhibit a power drift value of 2.3%, over > 30 min under free running conditions. The reduced stability of signal and idler wavelength generated from BIBO OPO can be attributed to the cavity length detuning. In addition, due to the high intra-cavity signal power as well as the green pump power, the thermal effects in the BIBO crystal lead to non-strict mode matching, which caused instability of the wavelength. Figure 5b shows the variation of the beam waist of the signal pulse in horizontal and vertical directions across the Rayleigh range of the focusing lens. The calculated beam quality factors M_x^2 and M_y^2 are 2.55 and 2.01, respectively. Due to the multiple roundtrips of the cavity for signal in the harmonically pumped geometry, such as spatial walk-off in the BIBO crystal, the M^2 are far from the diffraction limited. The noncollinear phase matching is a feasible method to improve the M^2 of signal. In the noncollinear phase matching geometry, the inherent decoupling of the pump pulse from the signal can be reduced in the crystal, causing the walk-off length to increase. This kind of scheme attempts to fully compensate for Poynting-vector walk-off using a noncollinear angle between the pump and signal pulse.

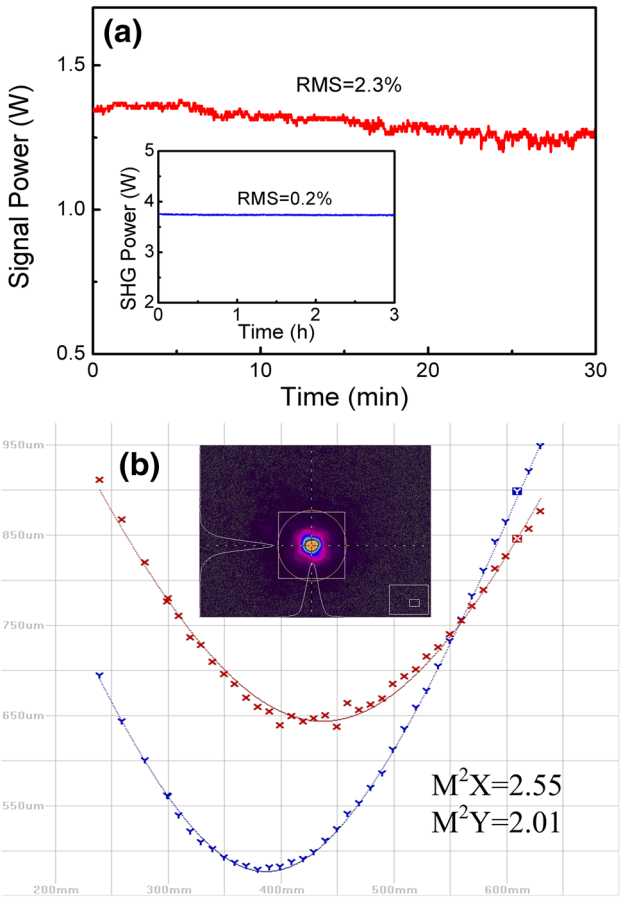

Fig. 5 **a** The long-term average powers stability of the pump and signal. **b** Spatial profile of the signal beam with maximum power

4 Conclusion

In summary, we have demonstrated a broadly tunable femtosecond BIBO OPO harmonically pumped by a frequency-doubled mode-locked Yb:KGW laser. Harmonic pumping is used to increase the repetition rate to 755-MHz, which is tenth-order harmonic repetition rate of the pump source. By rotating the angle of BIBO and optimizing the cavity length, the OPO is tunable across the 693–1000 nm in the signal range and 1100–2000 nm in the idler. With 3.75 W green pump power, the maximum output power of signal at 746 nm as high as 1.34 W is achieved, and the idler power is 408 mW at 1663 nm, respectively. Using a pair of prisms to compensate the extra-cavity dispersion, the pulse duration of the signal at 722 nm is 67 fs and the typical pulse duration of idler is 86 fs at 1580 nm. Under free operating conditions, the average power stability of signal at maximum power is less than 2.3% during 30 min. Future works will be focused on improving the repetition rate by optimizing the structure of cavity for achieving a few GHz operation. In addition, more signal output power is possible by increasing the pump energy such as using thin disk lasers. Such a high-repetition rate, high-power, broadly tunable visible to near-infrared femtosecond laser source will be applied in many applications, such as multiple-photon state generation.

Acknowledgements We thank the funding supported by the Strategic Priority Research Program of Chinese Academy of Sciences (XDB16030200); National Natural Science Foundation of China (11774410, 61575217); National Key Scientific Instruments Development Program of China (2012YQ120047); Key Research

Program of Frontier Sciences of Chinese Academy of Sciences (KJZD-EW-L11-03).

References

1. T.F. Albrecht, J.H.H. Sandmann, J. Feldmann, W. Stolz, E.O. Göbel, H. Hillmer, R. Lösch, W. Schlapp, Appl. Phys. B **60**, 5 (1995)
2. P. Tzallas, E. Skantzakis, L.A.A. Nikolopoulos, G.D. Tsakiris, D. Charalambidis, Nat. Phys. **7**, 10 (2011)
3. T. Sekikawa, A. Kosuge, T. Kanai, S. Watanabe, Nature **432**, 7017 (2004)
4. K.N. Joo, S.W. Kim, Opt. Express. **14**, 13 (2006)
5. R. Danielius, A. Piskarskas, A. Stabinis, G.P. Banfi, P. Di Trapani, R. Righini, J. Opt. Soc. Am. B **10**, 11 (1993)
6. A. Dubietis, R. Butkus, A. Piskarskas, J. Sel, Top Quantum Electron. **12**, 2 (2006)
7. G. Cerullo, S. De Silvestri, Rev. Sci. Instrum. **74**, 1 (2003)
8. V. Petrov, F. Rotermund, F. Noack, J. Opt. A Pure Appl. Opt. **3**, 3 (2001)
9. S.W. McCahon, S.A. Anson, D.-J. Jang, T.F. Boggess, Opt. Lett. **20**, 22 (1995)
10. D.E. Spence, S. Wielandy, C.L. Tang, C. Bosshard, P. Günter, Appl. Phys. Lett. **68**, 4 (1996)
11. Q. Fu, G. Mak, H.M. van Driel, Opt. Lett. **17**, 14 (1992)
12. P.E. Powers, R.J. Ellingson, W.S. Pelouch, C.L. Tang, J. Opt. Soc. Am. B **10**, 11 (1993)
13. W.S. Pelouch, P.E. Powers, C.L. Tang, Opt. Lett. **17**, 15 (1992)
14. V. Ramaiah-Badarla, S.C. Kumar, A. Esteban-Martin, K. Devi, K.T. Zawilski, P.G. Schunemann, M. Ebrahim-Zadeh, Opt. Lett. **41**, 8 (2016)
15. D.T. Reid, C. McGowan, W. Sleat, M. Ebrahimzadeh, W. Sibbett, Opt. Lett. **22**, 8 (1997)
16. P.J. Phillips, S. Das, M. Ebrahim-zadeh, Appl. Phys. Lett. **77**, 469 (2000)
17. J. Jiang, T. Hasama, Jpn. J. Appl. Phys. **41**, 3 (2002)
18. R. Hegenbarth, A. Steinmann, G. Tóth, J. Hebling, H. Giessen, J. Opt. Soc. Am. B **28**, 5 (2011)
19. T. Lang, T. Binhammer, S. Rausch, G. Palmer, M. Emons, M. Schultze, A. Harth, U. Morgner, Opt. Express. **20**, 2 (2012)
20. Z. Zhang, D.T. Reid, S.C. Kumar, M. Ebrahim-Zadeh, P.G. Schunemann, K.T. Zawilski, C.R. Howle, Opt. Lett. **38**, 23 (2016)
21. X. Meng, Z. Wang, W. Tian, H. He, S. Fang, Z. Wei, Opt. Lett. **43**, 4 (2018)
22. N. Coluccelli, D. Viola, V. Kumar, A. Perri, M. Marangoni, G. Cerullo, D. Polli, Opt. Lett. **42**, 21 (2017)
23. J. Vengelis, I. Stasevicius, K. Stankeviciute, V. Jarutis, R. Grigonis, M. Vengris, V. Sirutkaitis, Opt. Commun. **338**, 1 (2015)
24. X. Meng, Z. Wang, W. Tian, S. Fang, Z. Wei, Appl. Phys. B. **124**, 9 (2018)
25. C. Cleff, J. Epping, P. Gross, C. Fallnich, Appl. Phys. B. **103**, 4 (2011)
26. C. Gu, M. Hu, J. Fan, Y. Song, B. Liu, C. Wang, Opt. Lett. **39**, 13 (2014)
27. W. Tian, Z. Wang, X. Meng, N. Zhang, J. Zhu, Z. Wei, Opt. Lett. **41**, 21 (2016)
28. A. Esteban-Martin, Handbook of Optics, Chapter 22 pp. 22.1–22.72